Available online at www.sciencedirect.com
ScienceDirect
Journal of Power Sources 177 (2008) 566–578
JOURNAL OF POWER SOURCES
www.elsevier.com/locate/jpowsour

Battery switch array system with application for JPL's rechargeable micro-scale batteries

Mahmoud Alahmad [a,*], Herb Hess [a], Mohammad Mojarradi [b], William West [b], Jay Whitacre [b]

[a] *University of Idaho, Moscow Idaho 83843, USA*
[b] *Jet Propulsion Laboratory, California Institute of Technology, Pasadena, CA 91109, USA*

Received 14 September 2007; received in revised form 8 November 2007; accepted 9 November 2007
Available online 23 November 2007

Abstract

A battery switch array system is developed for solid-state rechargeable micro-scale lithium batteries, designed and developed by Jet Propulsion Laboratory (JPL), California Institute of Technology, for aerospace applications. The heart of the system is a topology unique in its dynamic reconfiguration ability by providing selective connection and isolation and versatile in its core design by incorporating passive, active or energy storage elements. It allows up to *N*-batteries to be connected in any desired configuration; providing maximum voltage, maximum capacity and a voltage/capacity ratio. This battery switch array system is part of a power management system that is developed to utilize these features and provide for multiple charging algorithms, real time status information and fault tolerant capabilities. A two microbattery prototype circuit is built using a microprocessor-based controller for verification of the system design and its features. The topology and its features will be explored in this paper to provide methods for modular and scalable energy storage system design.

Keywords: Battery; Battery scheduling; Battery system; Microbattery; Power management; Reconfigurable architecture

1. Introduction

Recent development in low power electronics and components to miniaturize spacecraft applications has led to the development of micropower sources. Jet Propulsion Laboratory (JPL) California Institute of Technology has been pursuing power generation, power storage and power conversion development. In the area of power storage, JPL has developed an all solid-state rechargeable micro-scale lithium ion battery cell (microbattery) rated at 4.25 V, with nAh capacity, where Ah (ampere-hour) is the unit used in specifying the capacity of a battery. The specific capacity of the microbattery at fabrication is based on the size of the active material used, ranging from 50 μm × 50 μm to 600 μm × 600 μm, to provide fabricated batteries with fixed capacities ranging from 1 to 200 nAh respectively. Fig. 1 shows samples of packaged integrated-circuit microbatteries developed by JPL. The figure shows three packages each with nine individual cells, encapsulated using parylene coating via a chemical vapor deposition (CVD) process for protection. The microbattery has been documented for its novel features, advantages and its potential to provide nanopower for highly integrated systems in aerospace applications [1–2].

One of the many advantages of the micro battery development is the ability to fabricate many microbatteries adjacent to each other in the same wafer. Approximately 20,000 individual microbattery cells are fabricated on a 4-in. silicon wafer. This fabrication leads to connecting adjacent microbatteries in series or in parallel. This connection can be incorporated during the fabrication phase as shown in Fig. 2. The figure shows the micrograph of five series cells. The outer squares are pads for electrical contact and the overlapping smaller squares are the active sections (area) of the battery. The active area shown in the figure is

* Corresponding author at: University of Nebraska-Lincoln, 206A, PKI, 1110 S. 67th Street, Omaha, NE 68182, USA. Tel.: +1 402 554 3527; fax: +1 402 554 2080.
E-mail addresses: malahmad2@unl.edu (M. Alahmad), hhess@ece.uidaho.edu (H. Hess), Mohammad.M.Mojarradi@JPL.NASA.GOV (M. Mojarradi), W.C.West@JPL.NASA.GOV (W. West), J.F.Whitacre@JPL.NASA.GOV (J. Whitacre).

0378-7753/$ – see front matter © 2007 Elsevier B.V. All rights reserved.
doi:10.1016/j.jpowsour.2007.11.053

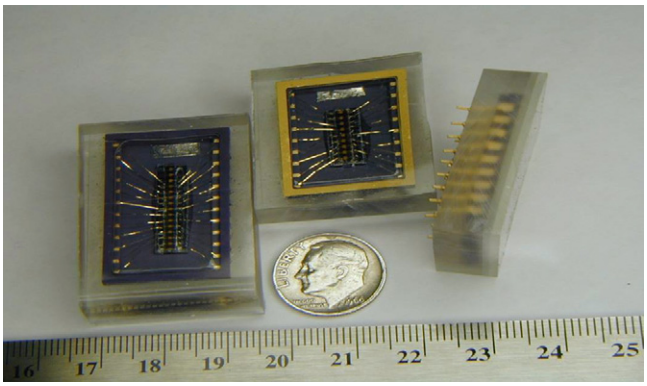

Fig. 1. Samples of three packaged integrated-circuit microbatteries with nine cells each developed by JPL. CVD parylene is used over the device and entire package.

for a 50 μm × 50 μm active area. Fabricating the microbatteries in a predetermined series and parallel connection will provide for desired voltage and capacity output, i.e. connecting ten cells in series will provide an output of 42.5 V with capacity of 50 nAh, using 50 μm × 50 μm active area for each cell. However, the predetermined connections will involve a customization process to provide for different voltages and capacities for different applications. Furthermore, additional balancing circuitry will be required to manage cells in series connected configurations during charging to eliminate overcharging and potential damage. Also, during discharge, series connected cells must be monitored to eliminate over discharge effects. In addition, faulty cells in the open or short circuit conditions, depending on their location within the prefabricated configuration could result in rendering entire portions of prefabricated battery system dead, resulting in removing a portion of otherwise good cells. This is similar to standard commercial battery pack (system) design with many internal hardwired cells, however, for these systems the number of cells is limited and the control and safety components are included as part of the pack.

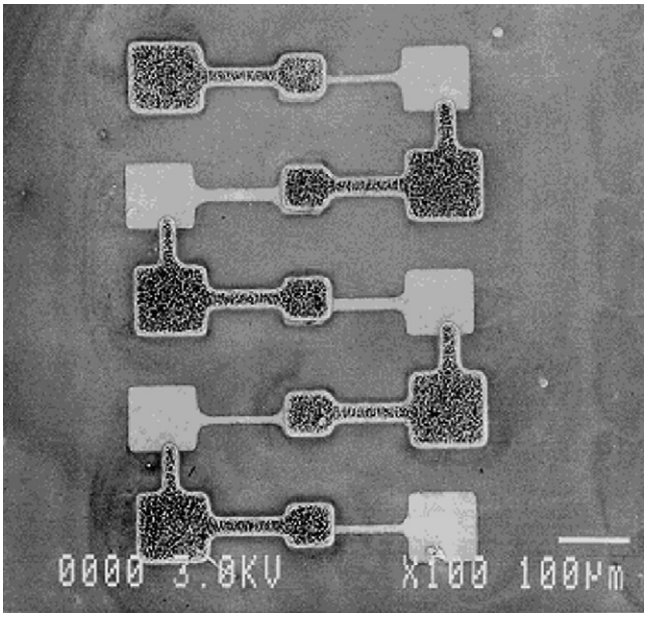

Fig. 2. A micrograph of five microbatteries connected in series. The outer squares are pads for electrical contacts and the overlapping smaller squares are the active sections of the battery.

While the predetermined connection for the cells is an approach that can be considered with added circuitry incorporated to meet the design safety and control requirements, a flexible design that is able to treat the cells as an active component in the design parameters to achieve an energy level that is scalable for different applications is more desirable. This is especially critical for space craft applications where flexibility, reconfiguration and remote control to alter a given state and make modifications to alter its output or activate its operation after a long period of rest (i.e. during flight time) is desirable and in some cases necessary. The ability to provide different voltages and capacities from the microbatteries after fabrication can lead to many benefits and applications as outlined in JPL's objectives to develop the microbattery [1–2], such as momentary CMOS memory back-up, voltage reference sources and for application related to System-On-a-Chip where the cells are mounted on the bottom of the IC. In addition, as the development of various microbattery systems expands and applications for its use in implantable medical devices and other areas grow, the need for greater and flexible voltages and capacities in a scalable and modular form will result in the development of novel ideas to address these issues. One of those novel ideas is the system described in this paper, which addresses the interconnection between the microbattery cells to provide for maximum flexibility in providing voltage and capacity in a scalable and modular approach.

Existing systems with this feature are limited. One of the methods [3] presented a synergetic battery pack configuration consisting of four series connected batteries. The terminals of each battery are provided with two switches to allow the positive and the negative terminal of the battery to connect to the charge or discharge bus. This connection allows for a single battery to be charged or discharged depending on the switch configuration. Also, the configuration allows for up to four batteries to be connected in series so that single battery, two series-connected batteries, three series-connected batteries or four series-connected batteries can be connected to the charge or discharge bus or terminal. Another method [4] presented the connection of eight secondary NiMH batteries; each rated 1.2 V, in series to provide 9.6 V output voltage. This voltage is used to power mobile robots. The paper discussed the option of having multiple packs of the series connected batteries so that once a pack is discharged it can be switched out and another pack switched in to provide the required voltage and capacity.

To meet the current and future needs of maximum flexibility, a switch array matrix architecture has been developed. This architecture is then further customized for the microbatteries with the development of the battery switch array system (BSAS) as part of comprehensive power management system. The BSAS theory of operation and features along with the power management system and the results of a prototype circuit built for verification will be presented.

This paper is organized as follows; Section 2 will present a brief description of the microbattery and its development. Section 3 will describe the switch array matrix architecture. Section

4 will provide an overview of the power management system and provide a detail discussion of the BSAS theory of operation, features t and simulation results. Section 5 will discuss and provide results from a prototype circuit developed to verify the system operations. Finally, Section 6, will provide a summary of this paper.

2. Microbattery background

JPL has been pursuing miniaturized power sources to accommodate proposed NASA missions that call for the use of smaller compact vehicles. These vehicles are used in a great variety of environments. As a result, devices developed for this specific application should take into account cold, hot, high radiation and sun-obscured environments and long life characteristics. In the area of power storage, JPL has used the Oak Ridge National Laboratories (ORNL) thin-film battery development [5–7] as template for the microbattery design. Several modifications were incorporated to facilitate the micro fabrication process to develop an all solid-state micro-scale lithium battery [1–2,8]. The developed micro-scale battery consists of lithium phosphorous oxynitride (LIPON) solid electrolyte, LiCoO2 cathode and two types of anode – thermally evaporated Li anode or sputtered Ni or Cu blocking anode film that serves as a substrate for in situ Li plating during charging.

The solid-state micro-scale batteries are characterized by having a solid electrolyte. This solid electrolyte is made using LIPON. The footprint of the developed batteries range from 50 μm × 50 μm to 600 μm × 600 μm given rise to capacity in the range of 1–200 nAh. A total of 20,000 batteries have been fabricated on a 4″ silicon wafer in 6 h of process time. Fig. 3 shows a schematic outline of the fabrication process and proceeds as follows [1,2]:

(a) On a silicon (Si) substrate, a 2 μm low-stress silicon nitride film is deposited to provide electrical isolation between microbattery cells as shown in Fig. 3a.
(b) The substrates are patterned with negative photo-resist to define the cathode current collectors.
(c) On the patterned photo resist, a Ti/Pt film is deposited. The wafer was then immersed in acetone or photo-resist stripper to remove the photo-resist and lift off the access Ti/Pt film. This defines the cathode current collectors as shown in Fig. 3b.
(d) The substrates were again patterned with negative resist to yield an opening in the photo-resist. A film of LiCoO2 was sputtered over the photo-resist and the wafers were immersed in acetone to remove the photo-resist and lift off the excess LiCoO2 to define the cathodes as shown in Fig. 3c.
(e) A solid electrolyte film (LIPON) film is deposited over the substrate to a thickness of 500–2000 nm.
(f) A Ni blocking anode film is deposited on the solid electrolyte film to protect it from reaction with ambient moisture during the removal from the chamber and further photolithography steps.
(g) The Ni film was patterned with positive photo-resist, then ion milled to define the Ni anode current collectors and contact pad as shown in Fig. 3d.
(h) Wafers are then patterned with negative resist to open via in the solid electrolyte over the cathode contact pads. Fig. 3e shows the unpassivated full cell microbattery.
(i) An encapsulation film is incorporated into the cell design as shown in Fig. 3f.

The process allows for permanent series connected cells via hardware during the fabrication. This is done by opening a via to the cathode current collector after the deposition of the electrolyte. Deposition and patterning of the Ni film is then performed. Table 1 shows a summary of the microbattery parameters [1,2,9]. The 50 nAh capacity shown is for cells provided for analysis and design, however, by varying the active area, JPL is able to develop batteries with other fixed capacities as indicated earlier. The "*C*" rate in the table refers to the charge–discharge rate of the microbattery, expressed in terms of its total storage

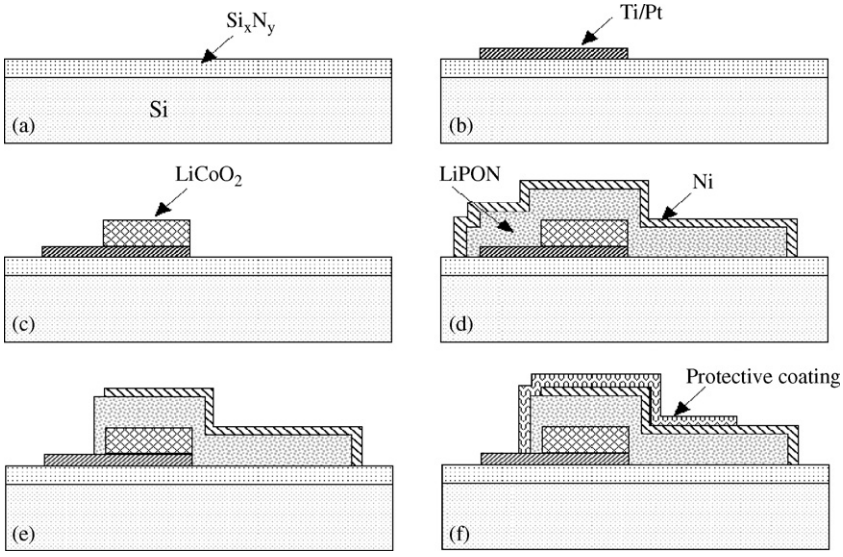

Fig. 3. Microbattery fabrication process.

Table 1
Micro-scale battery characteristics

Capacity	50 nAh
Voltage rating	
Rated	4.25 V
Cut off	3 V
Maximum overcharge	4.3–4.4 V
Electrical breakdown	5.5 V
Operating range	4.25 V–3 V
Deep discharge	0 V
Charge–discharge rating	
Rate of charge	0.1*C* to 10*C*
Efficient rate	0.1*C* to 0.15*C*
Normal rate	1.0*C*

capacity in nAh. The table provide for three different charge rates. The rate of charge is the range of charge that can be applied to the cells without damage. However for optimal utilization the standard (efficient) rate of 0.1*C*–0.15*C* should be used for an optimal state of health (SOH) and state of charge (SOC) parameters. The normal 1*C* rate shown is the minimum rate used to charge the battery at the laboratory due to equipment limitations (50 nA is used to charge the cells.)

3. Switch array matrix architecture

The switch array matrix (SAM) architecture is a generic topology that can be customized to fit many applications. Fig. 4 shows a schematic diagram of this topology for *N* elements (*N* + SAM) and consists of the following components:

1- Up to an *N* number of interrelated devices.
2- Up to an *M* number of Controllable elements.
3- Internal terminals (terminal one and terminal two).
4- External terminals (input port and output port).

The devices, the heart of the matrix, are able to be combined in different configurations to provide greater output, capacity or range than one element can provide. Typical devices include: primary and secondary cells within a battery pack; secondary microbatteries; individual primary and secondary commercial batteries; power sources; resistors; capacitor; light emitting diodes; memory elements and other devices. The controllable elements are switches that can be controlled for on/off operation to provide features for connecting adjacent devices in any user defined configuration. This controllability provides the devices with the option for parallel, series or parallel/series connection. In addition, any device can be isolated from the rest of the system. The topology requires a total of $[(4N) - 3]$ switches; were *N* is the number of elements in the topology. The selection of the switches is dependent on the technology and application being implemented. Examples of switches include relays, contactors, bulk and integrated NMOS, PMOS and CMOS transistors and MEMS switches.

The internal terminals, called terminal one and terminal two, are used to provide a connection from the equivalent device configuration to the external terminals. This equivalency can be a single device, or up to an *N* devices in series, parallel or series parallel configuration. The type of the terminals is dependant on the device used. For example, using battery storage devices will result in terminal one being the positive terminal and terminal two being the negative terminal, or vice versa. Finally, The external terminals, called an input port and an output port, are used to provide connection of the topology to external systems. The ports are interchangeable, depending on the devices used in the topology and what is being implemented. Two switches are provided at each port to control the connection of the ports to the internal terminals. Depending on the devices and application used, connection of the input port and output port to the internal terminals at the same time may not be allowed.

Reconfigurable architectures are of great interest to system designers. This interest is gaining more momentum as technology advances and system components become more modular allowing for design flexibility and innovative discoveries. This flexibility can be further enhanced by integrating diverse components with common objective. The modularity of this matrix can be seen in Fig. 5. The figure shows how to scale the architecture to provide for full modular design in terms of similar components with common function such as energy by using different cell capacities or different chemistry cells. Technol-

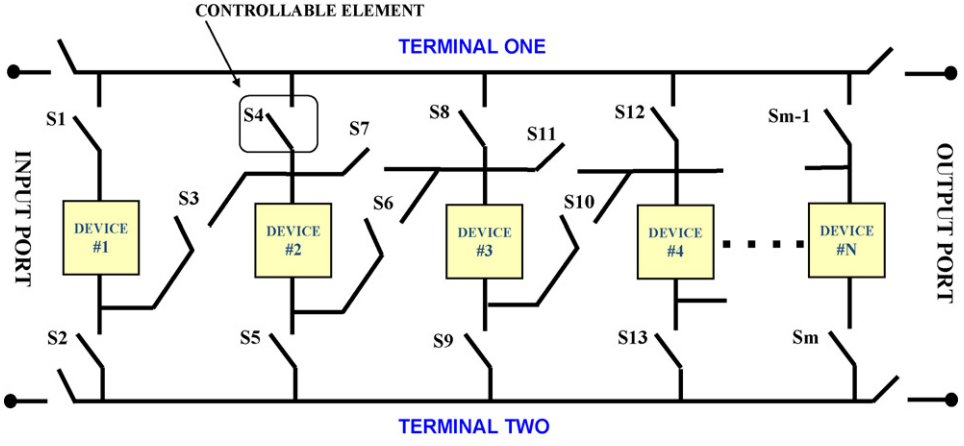

Fig. 4. Schematic diagram for the *N* + SAM topology with *N*-elements.

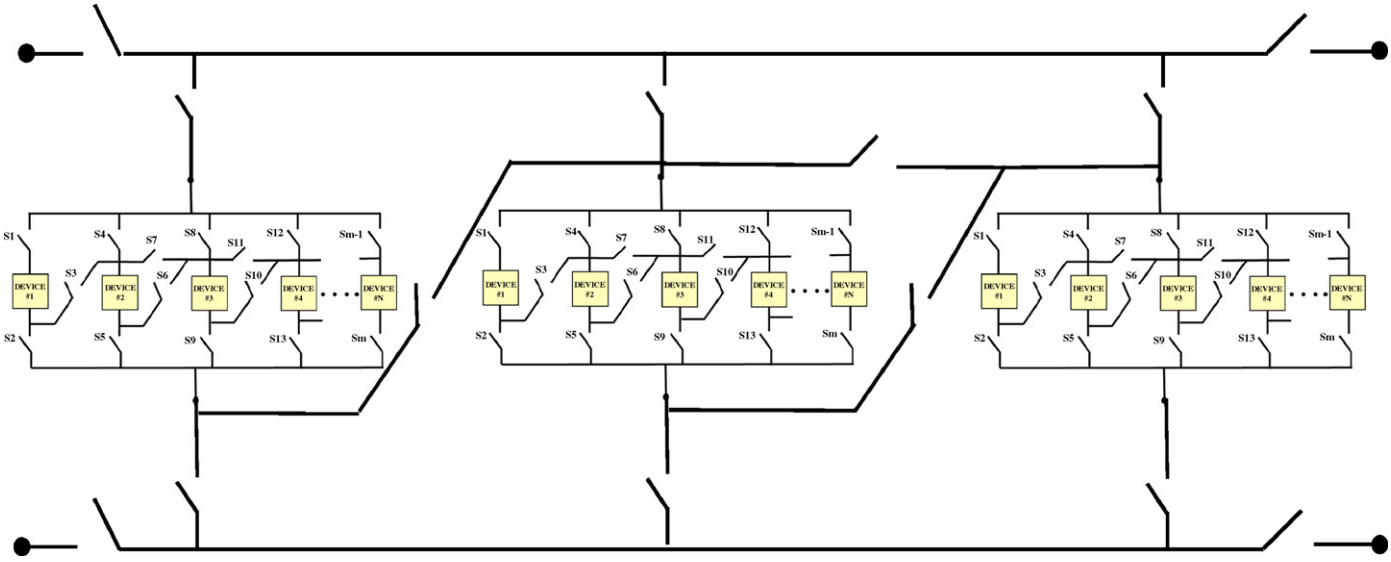

Fig. 5. Scalability and modularity of the architecture.

ogy and device limitations in any given application will be the barriers for expanding such architecture.

4. Switch array matrix architecture with applications For JPL's rechargeable battery

The $N+$SAM has been incorporated into a novel battery power management system (BPMS) to utilize the SAM features and provide additional features including multiple charging algorithms (constant current constant voltage (CCCV), pulse, etc.) for charging batteries individually or while connected in parallel. Real-time fault tolerant including detection and isolation as well as status information regarding the number of batteries charged, waiting to be charged, or faulty batteries are also provided. The operation of the system for this development is based on manual/remote operation to control the output voltage and capacity, hence, during the system operation cells selected for connection to a given load will remain in that state until the batteries are completely discharge. A dynamic intelligent system is under consideration that includes optimization and dynamic selection and switching of cells based on SOH, SOC and load requirements. A system block diagram of the BPMS is shown in Fig. 6. This system consists of a charge circuitry, a charge controller, a battery switch array system, an I/O interface circuitry, and a microprocessor-based controller. The charge circuitry is a system that provides 15 different current values in increments of 50 nA and a constant voltage level of 4.25 V [10]. The current increments and/or constant voltage can be selected to charge the battery as required by the system. The charge controller provides additional charge flexibility to the user by allowing variable pulse charging to be incorporated into the charging mechanism [11]. The I/O interface circuitry is a system component that allows the microprocessor controller to communicate with the individual circuits of the BPMS. The controller is a software/hardware microprocessor-based system that monitors

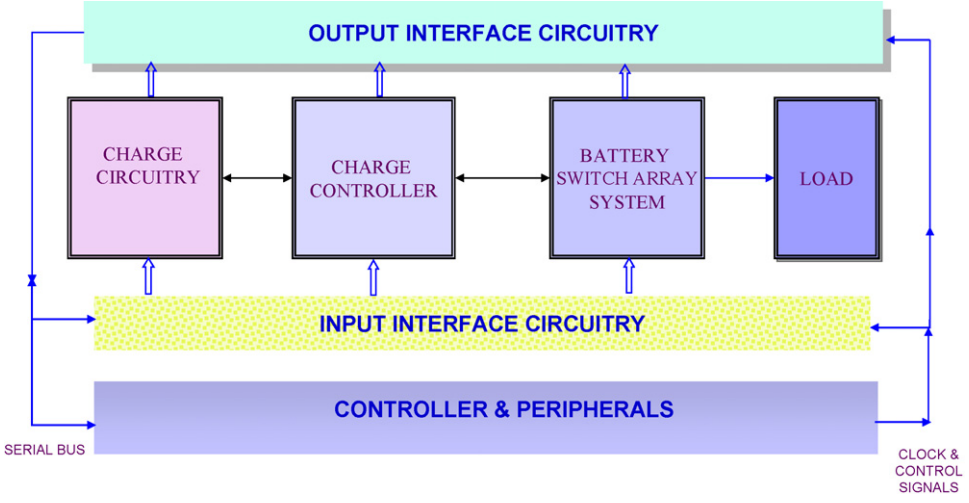

Fig. 6. BPMS block diagram.

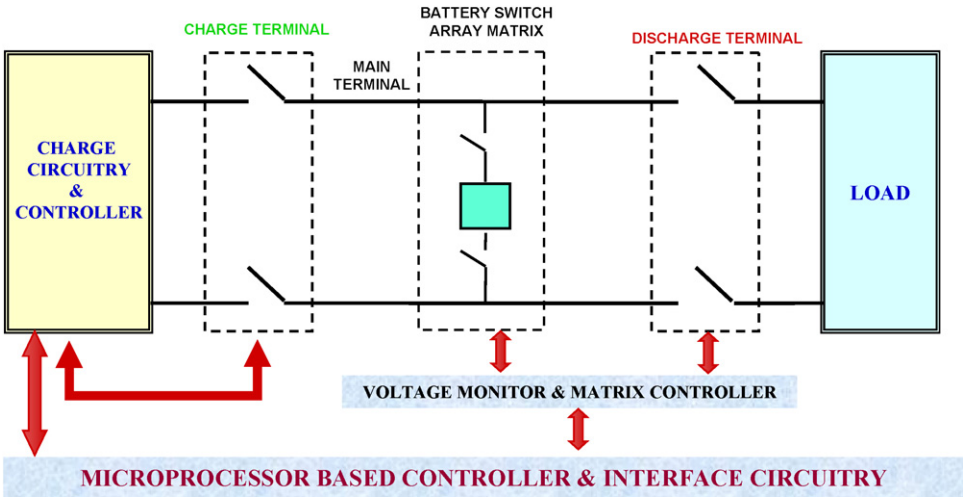

Fig. 7. Detailed BPMS with components of BSAS indicated.

and controls the operation of the individual components. The BSAS consists of three parts as shown in Fig. 7: battery switch array matrix, voltage monitoring circuit and matrix controller.

4.1. Battery switch array matrix

The matrix architecture has been customized for the JPL microbattery, called $N+$battery switch array matrix ($N+$BSAM.) The system capabilities allow for programmable voltage, programmable capacity, programmable voltage/capacity ratio and battery isolation. An advantage of the $N+$BSAM is its versatility to accommodate any number of batteries, depending on the application and technology used. The limitations will be based, in general, on the switches and their maximum voltage and current capabilities. To illustrate the features of this topology, four microbatteries will be used requiring an array of 13 switches. Each microbattery is rated 4.25 V and 50 nAh capacity.

4.1.1. Programmable voltage output

The $N+$BSAM can be configured to provide programmable voltage output: 4.25, 8.5, 12.75 and 17 V. The capacity for each of the selectable voltages is 50 nAh. Fig. 8 shows the configuration with all the batteries connected in series. In this example, switch number S1, S3, S6, S10 and S13 are closed to provide path from the positive terminal to the negative terminal. The charge terminal or the discharge terminal can be activated to charge or discharge the system. To provide a 4.25 V at the output, switch S1 and S2 can be closed to connect battery No.1 to the positive–negative terminal. In a similar configuration switch S4 and S5 will connect battery No. 2 to the positive–negative terminal. To provide 8.25 V, the first and second batteries are connected in series by closing switch S1, S3 and S5. With all batteries connected in series, the voltage between the positive–negative terminals is 17 V. This voltage is equivalent to the sum of all the individual battery voltage. Table 2 provides all available options and required switching arrangement for each voltage level.

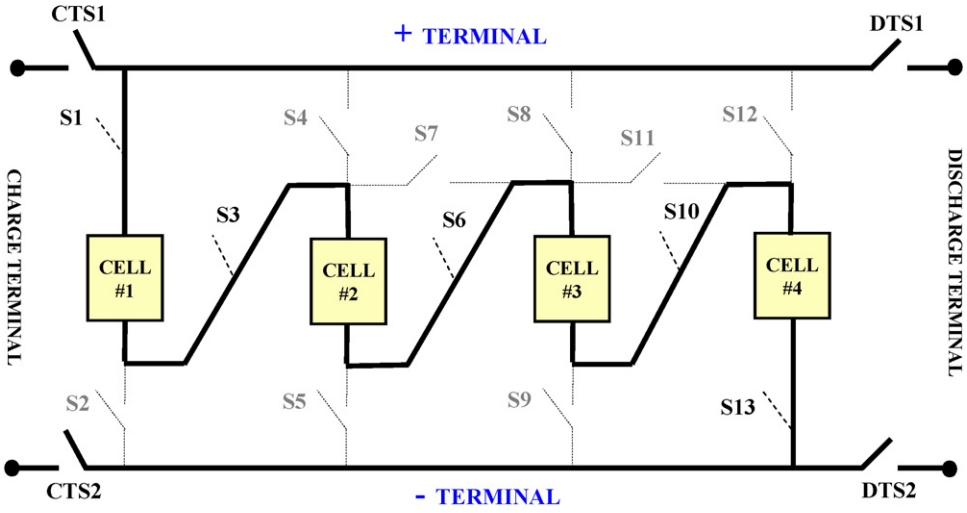

Fig. 8. 4-BSAM with all batteries connected in series.

Table 2
Programmable voltage output and switch connection (50 nA output)

Battery	4.25 V	8.5 V	12.7 V	17 V
B1	S1, S2	–	–	–
B2	S4, S5	–	–	–
B3	S8, S9	–	–	–
B4	S12, S13	–	–	–
B1 series B2	–	S1, S3, S5	–	–
B1 series B3	–	S1, S3, S7, S9	–	–
B1 series B4	–	S1, S3, S7, S11, S13	–	–
B2 series B3	–	S4, S6, S9	–	–
B2 series B4	–	S4, S6, S11, S13	–	–
B3 series B4	–	S8, S10, S13	–	–
B1 series B2 series B3	–	–	S1, S3, S6, S9	–
B1 series B2 series B4	–	–	S1,S3,S6,S11,S13	–
B1 series B3 series B4	–	–	S1, S3, S7, S10, S13	–
B2 series B3 series B4	–	–	S4, S6, S10, S13	–
B1 series B2 series B3 series B4	–	–	–	S1, S3, S6, S10,S13

4.1.2. Programmable capacity output

The $N+$BSAM can be configured to provide programmable capacity output: 50, 100, 150 and 200 nAh. The voltage at each of the selectable capacities is 4.25 V. A 4-BSAM with all the batteries connected in parallel to a load to provide 200 nAh is shown in Fig. 9. In this example, switch number S1, S2, S4, S5, S8, S9, S12 and S13 are closed to provide path from the positive terminal to the negative terminal. With all batteries connected in parallel, the output voltage at the discharge terminals is the same as the rated voltage across each battery i.e. 4.25 V; however capacity output is the sum of the individual capacities. Table 3 shows the required switching arrangement for each capacity level.

4.1.3. Programmable voltage/capacity ratio output

The $N+$BSAM also provide the user with a programmable voltage to capacity ratio output. Fig. 10 shows a 4-BSAM with two sets of two series connected batteries in a parallel configuration to provide 8.5 V with 100 nAh capacity at the output. In this example, switch number S1, S3, S5 provide the series connection for the first two batteries and also connection from the positive terminal to the negative terminal. In a similar manner, switch number S8, S10 and S13 provide the series connection for the second two batteries and also connection from the positive terminal to the negative terminal. Using six batteries in the BSAM example, 8.5 V, with 150 nAh capacities and 12.75 V, with 100 nAh capacities can be achieved. This feature provides greater flexibility as the number of batteries in the BSAM increases.

4.1.4. Programmable battery isolation

The $N+$BSAM provides the ability to isolate any battery, such as a faulty battery, from any desired configuration. This feature allows a power management system to test the system, and provide fault detection and isolation and hence provide fault tolerant capabilities. The system also can select specific batteries to be included or excluded from the configuration. This allows for battery ranking in terms of life cycle and operation performance to be implemented as part of the system. Fig. 11 shows a 4-BSAM with the first, second and fourth battery connected in series and the third battery disconnected from the system. In this example, switch number S1, S3, S6, S11 and S13 are closed to provide path from the positive terminal to the negative terminal with the third battery isolated. The voltage output in this configuration is 12.75 V with 50 nAh capacity.

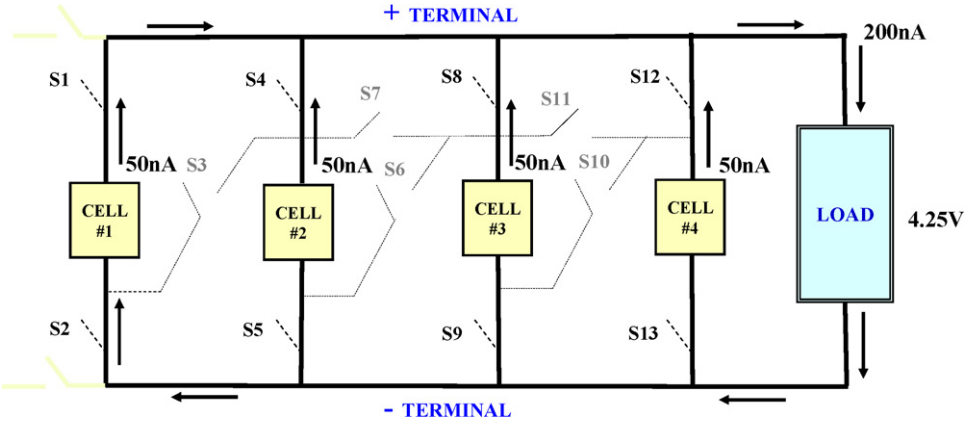

Fig. 9. 4-BSAM with all batteries connected in parallel.

Table 3
Programmable capacity output and switch connection (4.25 V output)

Battery	50 nAh	100 nAh	150 nAh	200 nAh
B1	S1, S2	–	–	–
B2	S4, S5	–	–	–
B3	S8, S9	–	–	–
B4	S12, S13	–	–	–
B1 parallel B2	–	S1, S2, S4, S5	–	–
B1 parallel B3	–	S1, S2, S8, S9	–	–
B1 parallel B4	–	S1, S2, S12, S13	–	–
B2 parallel B3	–	S4, S5, S8, S9	–	–
B2 parallel B4	–	S4, S5, S12, S13	–	–
B3 parallel B4	–	S8, S9, S12, S13	–	–
B1 parallel B2 parallel B3	–	–	S1, S2, S4, S5, S8, S9	–
B1 parallel B2 parallel B4	–	–	S1, S2, S4, S5, S12, S13	–
B1 parallel B3 parallel B4	–	–	S1, S2, S8, S9, S12, S13	–
B2 parallel B3 parallel B4	–	–	S4, S5, S8, S9, S12, S13	–
B1 parallel B2 parallel B3 Parallel B4	–	–	–	S1, S2, S4, S5, S8 S9, S12, S13

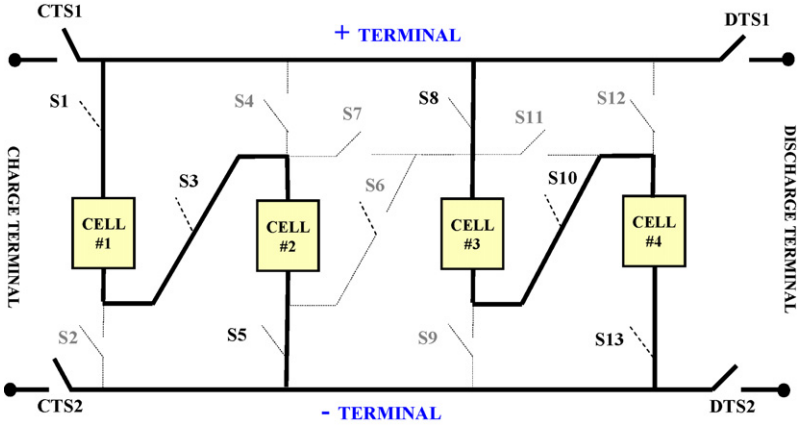

Fig. 10. 4-BSAM connection for voltage/capacity output ratio.

4.1.5. Dynamic scheduling feature

Multiple batteries are being incorporated to handle the increasing energy demand of equipment and systems. The Compaq Ipaq PDA is equipped with an add-on module that contains pcmcIA expansion and an auxiliary battery pack. Similarly, the HP omniBook 500 notebook when latched to its docking station is powered by a 11.1 V, 3100 mAh primary battery and two 14.8 V, 3400 mAh secondary batteries that enable plugged in and out independently [19]. Due to size and weight constraints this option is still in its infancy. However for some applications, it is a desirable option that increases the reliability and efficiency of the system. When multiple batteries are considered, smart man-

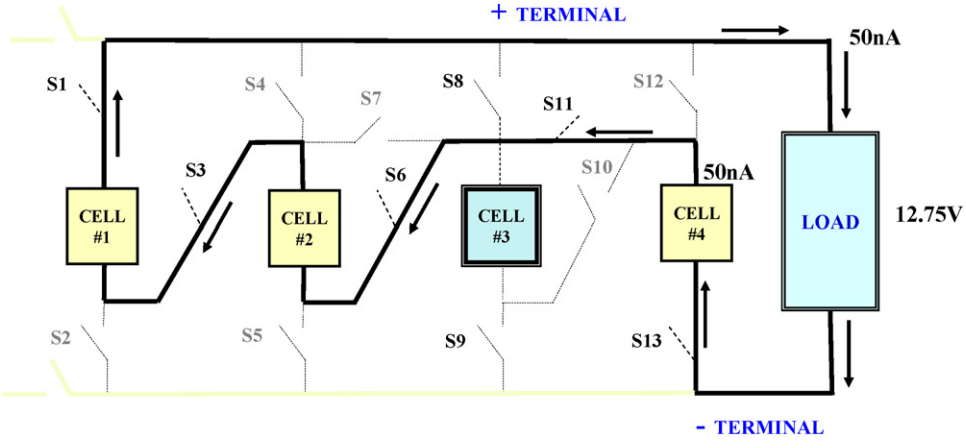

Fig. 11. 4-BSAM connection, with battery No. 3 isolated from the load.

agement policies are being integrated to enhance the operation of each battery in the system and increase its performance and operational life.

The $N+$BSAM can be used in applications where multi batteries are required to supply an increasing energy requirement. As the number of batteries increases, scheduling methods are adopted to use each battery effectively and efficiently. Existing scheduling methods include sequential, parallel, random, joint, threshold, dynamic, static or Round–Robin and heterogeneous method [13,14]. In the sequential method, each battery is fully discharged before the next battery in sequence is selected for discharge. In the parallel method, batteries are connected to the load alternatingly until all batteries are discharged. In the threshold method, each battery is discharged to a predetermined threshold and then the next battery in sequence is discharged similarly. A battery is not connected unless it has recovered above the threshold. In the static or Round–Robin method, each battery is discharged for a specified time interval, after which the next battery in sequence is connected for the same specified time interval. This will loop until all batteries are discharged. In the random method, each battery is discharged for a specified time interval, after which a random battery is connected for the same specified time interval. In the Joint method, *N*-batteries are connected to the load in parallel. Each battery sees 1/*N* of the load until all batteries are discharged. In the dynamic technique, each battery is selected based on output voltage, state of charge and elapsed discharge time. Finally, in the heterogeneous method, batteries of different capacities and discharge curves are used. Using the parallel and Round–Robin techniques in correlation, the best fit parameter of batteries can be chosen for different applications using non-uniform time intervals of connection to each battery.

This topology can be efficiently applied as novel method to provide for a dynamic adaptive battery selection. This is achievable since real time information on the status of each battery and a host of battery parameters can be monitored, including but not limited to: rate of charge, charge temperature, discharge temperature, rate of discharge, type of discharge, discharge time, cycle number, and depth of discharge. Type of discharge refers to the method used to discharge the cells via a constant voltage discharge, constant current discharge or constant power discharge [15].

4.1.6. Life cycle analysis feature

In addition to the scheduling feature, the life cycle of each battery are established. The rechargeable battery could be in one of the following states depending on the voltage measured across its terminals: undercharged, at a specific level within the charge–discharge boundary, fully charged, overcharged or faulty or nonfunctioning. A system tracking these stages is able to accurately indicate where each battery is in its charge–discharge, or standby cycle and use this information to provide a model for each battery to predict useful life, statistical information and for dynamic adaptive scheduling. The following voltage levels are used to categorize the microbattery in one of the following states or categories:

Table 4
Microbattery categorization table

CAT1	Deep discharge state (0 V $\leqq$ battery voltage <3 V)
CAT2	Discharge state (3 V $\leqq$ battery voltage <4.25 V)
CAT3	Top of charge state (4.25 V $\leqq$ battery voltage <4.5 V)
CAT4	Overcharged state (battery voltage $\geqq$ 4.5 V)
CAT5	Suspected faulty state (battery requiring further testing)
CAT6	Fully charged state (battery ready for utilization)
CAT7	Faulty state (battery is faulty, isolate)

1- <3 V as an undercharged microbattery requiring additional tests.
2- 3–4.25 V as the normal charge and discharge voltage level.
3- 4.25–4.50 V as a normal battery requiring additional charging.
4- >4.50 V as an overcharged microbattery possibly faulty in the open circuit condition.
5- Faulty microbatteries with open circuit or short circuit condition.

Based on these settings, the microbattery can be categorized and its current state identified as it moves in the charge, discharge and standby cycle. Table 4 shows a summary of the categorization method developed for the microbatteries. This information will provide the user with the number of microbatteries fully charged, these are the microbatteries located in CAT6; provide the number of microbatteries waiting to be charged (located in CAT2); provide the number of faulty microbatteries(located in CAT7) and so forth. The following describes each category and its relationship to the microbattery condition.

In Category 1 (CAT1), the microbattery voltage is less than three volts. This is a temporary category used for microbatteries that are undercharged, microbatteries that are in deep discharge or faulty microbatteries with short connection between the two terminals (anode and cathode). The microbatteries in this state are scheduled for predefined test by the system to increase their voltage to 3 V. Upon successful completion, they are placed in CAT2. If the microbattery voltage does not increase during the time limit, they are placed in CAT5 for further testing.

In Category 2 (CAT2), the microbattery voltage is greater than three volts but less than 4.25 V. This is a temporary category used for microbatteries with voltage rating that falls within normal settings of the normal charge discharge boundary. The microbatteries in this state are charged using predefined charging methods. If charging is successful, then the microbatteries are identified as fully charged and are placed in CAT6. If a faulty condition occurs and the voltage across the microbattery never reaches 4.25 V during a time limit, they will be placed in CAT5 for further testing.

In Category 3 (CAT3), the microbattery voltage is greater than 4.25 V but less than 4.5 V. This is a temporary category used to classify microbatteries with voltage rating that meet the condition for a fully charged microbattery. However, since the amount of charge available is not known, the microbatteries in this state are charged using a constant voltage charging method [15]. After a successful charging, the microbatteries are identified as fully charged and are placed in CAT6. If a faulty condition

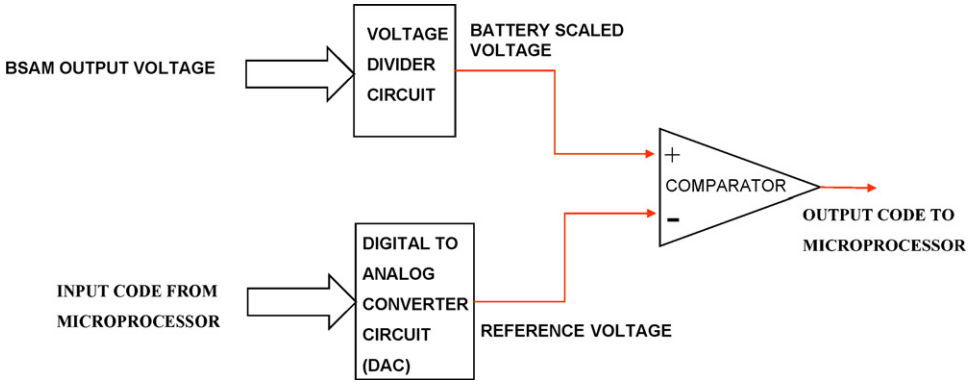

Fig. 12. Block diagram for the voltage monitor circuit.

occurs during charging, they will be placed in CAT5 for further testing.

In Category 4 (CAT4), the microbattery voltage is greater than 4.5 V. This is a temporary category used for microbatteries that are overcharged, microbatteries that are in deep overcharge or faulty microbatteries with open connection between the two terminals (anode and cathode). The microbatteries in this state are tested using a high pulse discharge method. If the voltage decreases below 4.25 V, the microbattery is placed back in CAT2 for further charging and categorization. If the test is unsuccessful and the voltage across the microbattery remains above 4.5 V, it is placed in CAT5 for further testing.

In Category 5 (CAT5), the microbattery could be experiencing unstable conditions with voltage level greater than 4.5 V or less than 3 V. This is a temporary category used to classify the microbattery as a suspected faulty microbattery. The voltage across the microbattery is unstable with a possible open or short circuit condition. Two additional tests are conducted to determine if the voltage reading across the microbattery is a temporary condition resulting in an under or over voltage condition. If the microbatteries, after the completion of the tests, are still experiencing the same behavior, they are classified as being permanent faulty microbatteries and they are placed in CAT7. On the other hand, if they show normal behavior, they will be placed in CAT2 for normal charging procedure.

In Category 6 (CAT6), the microbattery is classified as fully charged. This category is a permanent category with all the microbatteries eventually ending up in this category if they are functioning microbatteries. Once the discharging starts, the microbatteries are removed from his category and placed in their respective category to repeat the process. Finally, Category 7 (CAT7) is a permanent category with the microbattery classified as permanently faulty. The microbatteries in this category are identified for exclusion from the operation of the system.

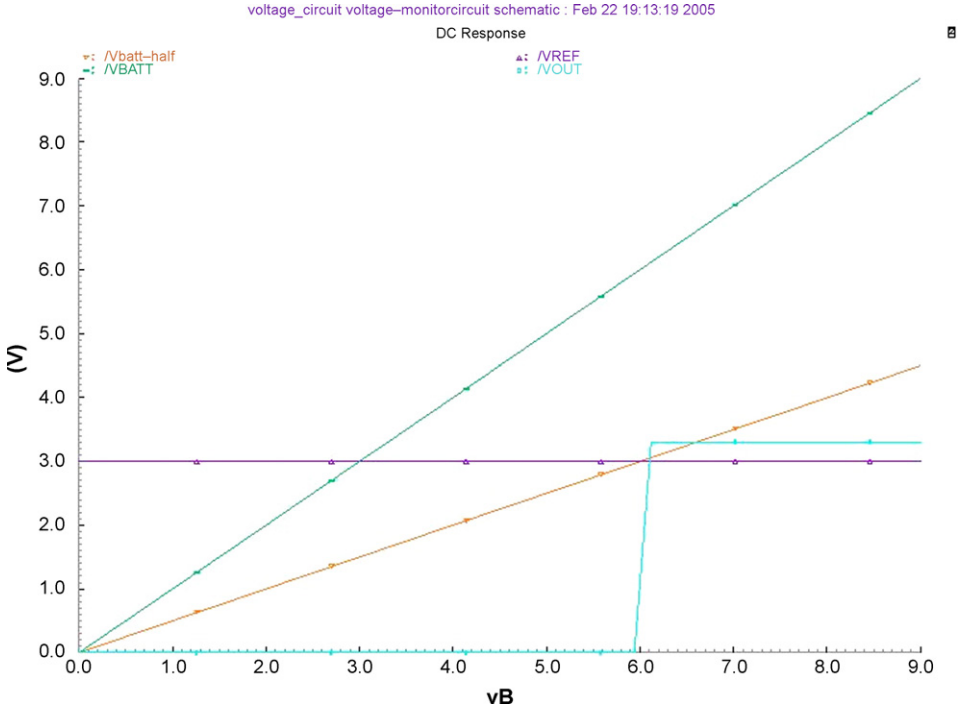

Fig. 13. Simulation results for the voltage monitor circuit, operation using a 3 V reference voltage.

The microbatteries will remain classified in this category with no additional testing. However, modifications can be made to allow for additional testing during predefined elapsed time settings.

4.2. Voltage monitor circuit

This circuit monitors the voltage of the $N+$BSAM during the discharge cycle and consists of a voltage divider circuit, a comparator and a digital to analog converter (DAC). Fig. 12 shows a block diagram of this circuit. The voltage divider circuit has one input from the discharge terminal representing the voltage across the microbatteries and one output that is 50% fraction of the input voltage to reduce the required voltage reference that needs to be generated by the DAC circuit. The circuit is designed using 3.3 V Microwave silicon on insulator (SOI) devices [16]. The current draw from the microbattery configuration to operate this voltage divider circuit should not exceed 1%. The total simulated current drawn from the source is 11fA, well below the maximum specified limit for this current. The DAC circuit provides the comparator circuit with the reference voltage as determined by the microprocessor-based controller. Due to the limitation of the devices and to reduce the DAC output, the values are monitored at a 50% range using the voltage divider circuit. A three-bit DAC circuit has been designed using an R-2R topology, without an OP-AMP, using SOI devices [17]. The resistors used in this circuit are P-WELL type resistors. This type of resistor is used to minimize the noise effect. The R-2R DAC is not a uniform DAC. The resistor values were selected to adjust the output voltage of the DAC to produce the required signal. The simulation results verified the operation of the circuit measuring an output of 2.99990 V and 1.49496 V when a 3 V and a 1.5 V reference voltage is requested respectively. The comparator circuit is used to compare the voltage of the microbatteries against the reference voltage. The output of the comparator circuit is monitored by the microprocessor-based controller to indicate that the lower discharge voltage limit across the microbattery

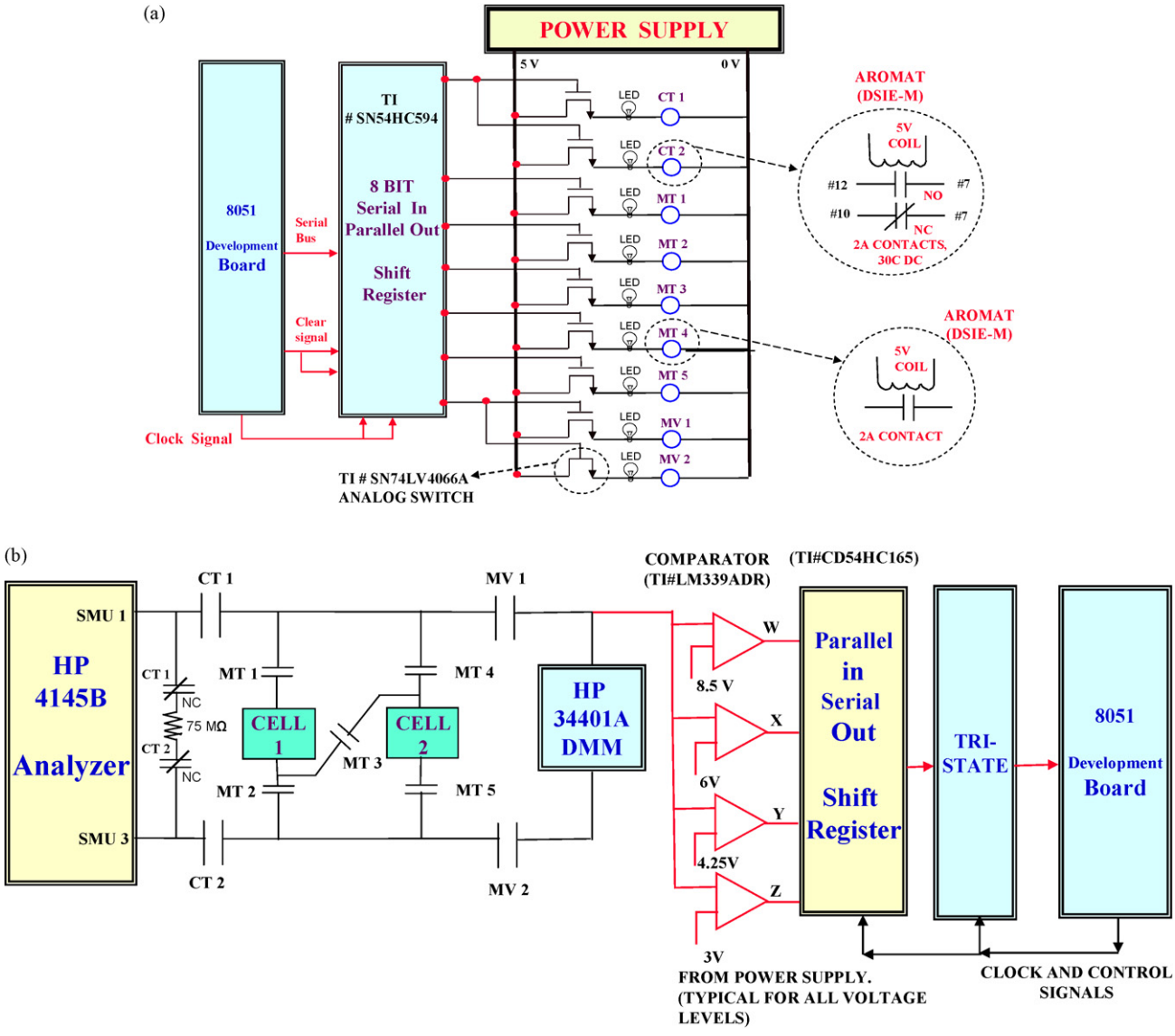

Fig. 14. Part a and part b comprise the prototype circuit for the BSAM.

configuration is reached. The microprocessor-based controller will then initiate the signal commands for the removal of the microbatteries from the discharge terminal.

The simulations for the complete voltage monitor circuit are carried out for a single microbattery and two microbatteries connected in series. For the first case, a 1.5 V reference voltage is generated and an input simulating the battery voltage is swept from 0 to 9 V. The simulation shows that the voltage monitor circuit generated the correct signal when the voltage reached 3 V, as shown in Fig. 13. Similar results are obtained for the series connected case.

4.3. Matrix controller

This circuit is the interface between the controllable elements in the $N+$BSAM and microprocessor-based controller. In other words, this circuit will implement the request of the controller to turn on or off the controllable elements in order for a given microbattery to be connected to its adjacent microbattery or to the charge–discharge terminal and so forth. For example, if the controllable elements are MOS transistors, then the matrix controller is a circuit that translates the input of the microprocessor-based controller into voltage and current signals to be applied to the gates of each transistor to turn them on and off for a specific configuration. The matrix controller for a two-microbattery integrated circuit using microwave silicon on insulator MOS transistors has been presented in [12,18]. Another implementation of the matrix controller uses relays as the controllable elements. The matrix controller controls voltage and current input to the coils of the relay. The activation of the relays will open or close contactors associated with each microbattery as will be discussed in the prototype circuit design in the next section.

5. $N+$BPMS implementation

The benefits of the $N+$SAM are explored in the customized system for the microbatteries. The system has been built using SOI devices and tested to verify its operation. Considerations for the overhead energy requirement for this system are not addressed. This is due to the fact that the research focus is on the exploration of novel methods to utilize the microbatteries and verification of those methods both at the IC level and at the prototype level. A 2-battery $N+$BPMS prototype circuit board has been built using standard components such as relays, shift registers, comparators, and an 8051 microprocessor controller. The latch-in electromagnetic relay is used as the controllable element providing isolation with minimum losses during microbattery connection to the system. The selected relay has an initial contact resistance of 50 mΩ and nominal power rating of 400 mW for the coil. However, for integrating the cells for IC applications, NMOS, PMOS and MEMES devices are used. The prototype circuit for the BSAM is shown in Fig. 14. With two microbatteries in the matrix topology, nine relays are used to provide various connections, such as MT3 representing the switch connecting the first microbattery to the second microbattery for series connection during discharge and so forth.

The CCCV is used to charge the cells with a constant current rated at 1C (50 nA) applied to the microbattery until the microbattery reaches rated voltage value. At rated voltage value (4.25 V), the constant current input is removed and a constant voltage equivalent to the microbattery rated voltage is applied across the microbattery. This voltage remains connected to the microbattery until the current supplied from the voltage source reaches approximately 5% of the rated 1C value (2.5 nA). The voltage source is then disconnected and the microbattery is defined as being fully charged [15]. Finally, the program for the microprocessor is written in "C" language. Modifications to this program are easily accomplished to accommodate user, data, battery type and other specifications.

The system has been tested with the JPL microbatteries. Test results verified that the operation of the circuit met the design objectives and verified the features of the $N+$BPMS system. For example, Fig. 15 shows the results obtained for parallel battery charge, then series discharge followed by a single discharge. At point A, the program measures the voltage across both batteries. Since both batteries were already charged from a previous test (categorized as being in CAT3 (Voltage greater than 4.25 V)),

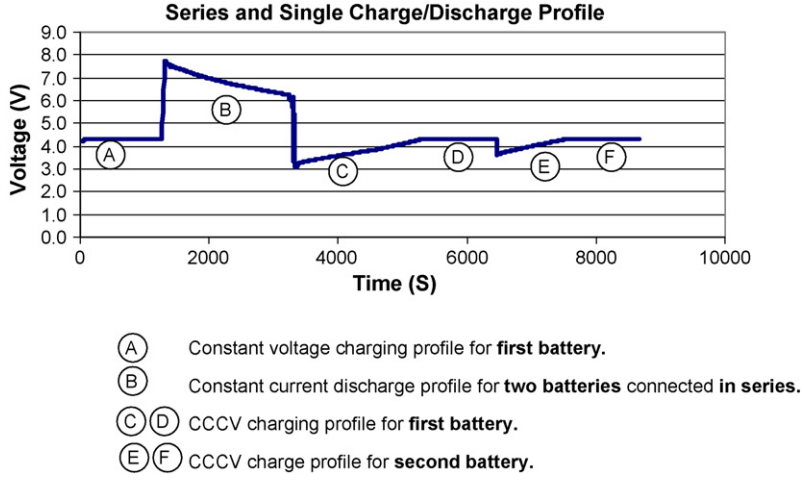

Fig. 15. Simulation results showing the charge–discharge–charge results for two series and single microbatteries.

the program applies Constant Voltage for the batteries connected in parallel for a predetermined amount of time. At point B, the data shows the choice chosen for discharge; the user selects a series discharge at 50 nA. The program is designed to terminate the series discharge at approximately 6 V. At points C, D, the system was set for single battery operation and charge at 50 nA for the first and second battery. The voltage graphs show the constant current portion of the results at point C and the constant voltage results at point D. At point E, F, single battery charge at 50 nA for the second battery takes place. The voltage graph show the constant current portion of the results at point E and the constant voltage results at point F.

6. Conclusion

A customized battery switch array system has been developed with applications for microbatteries developed by JPL. The battery switch array system allows up to *N*-batteries to be connected in any desired configuration. This flexibility allows for providing maximum voltage by connecting all batteries in series; providing maximum capacity by connecting the batteries in parallel; providing a voltage/capacity ratio by connecting the batteries in a parallel-series configuration. The modularity of the system can be explored with other devices as discussed. The system also provides for voltage monitoring via custom built subcomponent circuits. A two battery prototype circuit has been developed and tested to verify the design development and novel features of this system.

References

[1] W.C. West, J.F. Whitacre, E.J. Brandon, B.V. Ratnakumar, IEEE AESS Syst. Mag. 16 (8) (2001) 31–33.
[2] W.C. West, J.F. Whitacre, E.J. Brandon, B.V. Ratnakumar, J. Micromech. Microeng. 12 (2002) 1–5.
[3] Davis Amanda, M. Salameh Ziyad, S. Eaves Stephen, IEEE Trans. Energy Convers. 14 (3) (1999) 830–835.
[4] Andreas Birk, AI-lab, Vrije Unversiteit Brussel Belgium, Autonomous Recharging of Mobile Robots, Draft version (paper #97RO029) accepted at ISATA'97, Florence, 1997.
[5] X. Yu, J.B. Bates, G.E. Jellison, F.X. Hart, J. Electrochem. Soc. 144 (1997) 524.
[6] B. Wang, J.B. Bates, F.X. Hart, B.C. Sales, R.A. Zuhr, J.D. Robertson, J. Electrochem. Soc. 143 (1996) 3203.
[7] B.J. Neudecker, N.J. Dudney, J.B. Bates, J. Electrochem. Soc. 147 (2000) 517.
[8] J.F. Whitacre, W.C. West, E. Brandon, B.V. Ratnakumar, J. Electrochem. Soc. 148 (10) (2001) A1078–A1084.
[9] Private communications with W.C. West (JPL), J.F. Whitacre (JPL).
[10] B.B. Blalock, J. Jackson, A Microbattery Charger/Regulator System in SOI, Consortium of Universities Developing CMOS Integrated Circuits for Instruments and Sensors for NASA's Missions, Research Workshop, April 10th, 2003.
[11] F. Zghoul, An integrated pulse charging circuit for lithium micro scale batteries, Masters thesis, University of Idaho, 2003.
[12] V. Sukumar, M. Alahmad, K. Buck, H. Hess, H. Li, D. Cox, F.N. Zghoul, J. Jackson, S. Terry, B. Blalock, M.M. Mojarradi, W.C. West, J.F. Whitacre, J. Power Sources 136 (2) (2005) 401–407.
[13] R. Rao, S. Vrudhula, D. Rakhmatov, ISLPED'03, August 25–27, 2003.
[14] L. Benini, D. Bruni, A. Macii, E. MAcii, M. Poncino, IEEE Trans. Comput. 52 (8) (2003) 985–995.
[15] D. Linden, T.B. Reddy, Handbook of Batteries, third ed., 1998.
[16] Honeywell Microwave SOI Foundry Document, A Honeywell proprietary information.
[17] R.J. Baker, H.W. Li, D.E. Boyce, CMOS Circuit Design, Layout and Simulation, IEEE Press, 1998.
[18] V. Sukumar, M. Alahmad, et al., J. Analog Integr. Circuits Signal Process. 44 (3) (2005) 203–211.
[19] K. Lahiri, A. Raghunathan, S. Dey, D. Panigrahi, in: Proceedings of the 15th International Conference on VLSI Design(VLSID'02).